DOI: 10.1002/hlca.201900026

COMMUNICATION

HELVETICA chimica acta

Exploring Crystal Structure in Ethyne-Substituted Pentacenes, and Their Elaboration into Crystalline Dehydro[18]annulenes

Matthew J. Bruzek,[a] Emma K. Holland,[a] Anna K. Hailey,[b] Sean R. Parkin,[a] Yueh-Lin Loo,[b, c] and John E. Anthony*[a]

[a] Department of Chemistry/Center for Applied Energy Research, University of Kentucky, Lexington, Kentucky, 40511, USA, e-mail: anthony@uky.edu

[b] Department of Chemical and Biological Engineering, Princeton University, Princeton, New Jersey, 08544, USA

[c] Andlinger Center for Energy and the Environment, Princeton University, Princeton, New Jersey, 08544, USA

Dedicated to *François Diederich* on the occasion of his retirement.

Approaches to control the self-assembly of aromatic structures to enhance intermolecular electronic coupling are the key to the development of new electronic and photonic materials. Acenes in particular have proven simple to functionalize to induce strong π-stacking interactions, although finer control of intermolecular π-overlap has proven more difficult to accomplish. In this report, we describe how very weak hydrogen bonding interactions can exert profound impact on solid-state order in solubilized pentacenes, inducing self-assembly in either head-to-tail motifs with strong 2-D π-stacking, or head-to-head orientations with much weaker, 1-D π-stacking arrangements. In order to achieve 3-D π-stacking useful for photovoltaic applications, we elaborated a series of diethynyl pentacenes to their trimeric dehydro[18]annulene forms. These large, strongly interacting structures did indeed behave as acceptors in polymer photovoltaic devices.

Keywords: acenes, crystal engineering, organic photovoltaic, pentacenes, dehydroannulenes, annulenes.

Introduction

The self-assembly of aromatic chromophores – and the precise intermolecular and molecule-interface interactions enabled by the nature of the assembly – is a key factor in the electronic and photonic properties of organic crystals and films.[1] For example, development of materials for transistor applications, where charge transport must be maximized, benefitted from strategies that enhance π-stacking,[2] while materials for light-emitting diodes require complete disruption of aryl-aryl electronic interactions to maximize emissive yield.[3] In photovoltaics, the orientation of molecules at the donor/acceptor interface has been found to have profound impact on the efficiency of photo-induced charge transfer.[4] Even within these two disparate categories of intermolecular interactions subtle changes in intermolecular contacts can yield substantial changes in electronic coupling,[5] making control of self-assembly in these systems a critical handle to tune performance.

For nearly two decades, our research has focused on methods to control the solid-state order of acenes, a promising chromophore frequently used in the field of organic electronics.[6] Through a simple functionalization scheme, we were able to induce strong π-stacking interactions, enhance solubility, and increase stability in compounds such as pentacene.[7] More recently, we have tuned the acene chromophore to make it suitable for use as an acceptor in bulk-heterojunction organic photovoltaic devices, discovering that only certain crystalline assemblies yielded meaningful device performance.[8] Here, we discuss the subtle intermolecular interactions that yield promising crystalline motifs, as well as approaches to

Supporting information for this article is available on the WWW under https://doi.org/10.1002/hlca.201900026

enhance the three-dimensional electronic coupling between chromophores in the solid state necessary for photovoltaic applications.

As part of our effort to turn pentacenes into adequate acceptors for use with the hole-transporting polymer, poly(3-hexylthiophene) (**P3HT**) in organic photovoltaic (OPV) devices, we developed a series of derivatives substituted with electron-withdrawing groups.[9] In the case of the 2,3-dicyano pentacenes (**CN_2Pn**s), we noticed a consistent crystal-packing motif that was quite different from the arrangements we observe in the vast majority of pentacene derivatives we have prepared. Typically, the ends of the pentacene units are offset by slipping along the short axis (*Figure 1*, *top*). We observe this short-axis slip in a wide variety of silylethyne-substituted acenes, even those with a variety of substituents (*e.g.*, methyl, nitro, and halogen) at the 'end' (2,3 or 9,10) positions. This short axis slip is one factor inhibiting the charge carrier transport efficiency in silylethyne functionalized acenes, as it prevents direct overlap of the acene chromophore in 2D π-stacked arrangements. In the dicyano system (*Figure 1*, *bottom*), this short-axis slip is completely eliminated, leading to the acenes arranging in a 1D 'tape' motif. The aromatic C–H groups are geometrically compatible with the splay of the dicyanoarene group of the adjacent molecule. Literature suggests that there is likely a degree of C–H-π interaction between the aromatic proton and the π bonds of the nitrile, supported here by contacts as close as 2.01 Å between the aromatic hydrogen and the nitrogen atom of the nitrile group, well within the range (1.7 Å – 2.6 Å) seen in other nitrile hydrogen-bonding arrangements.[10]

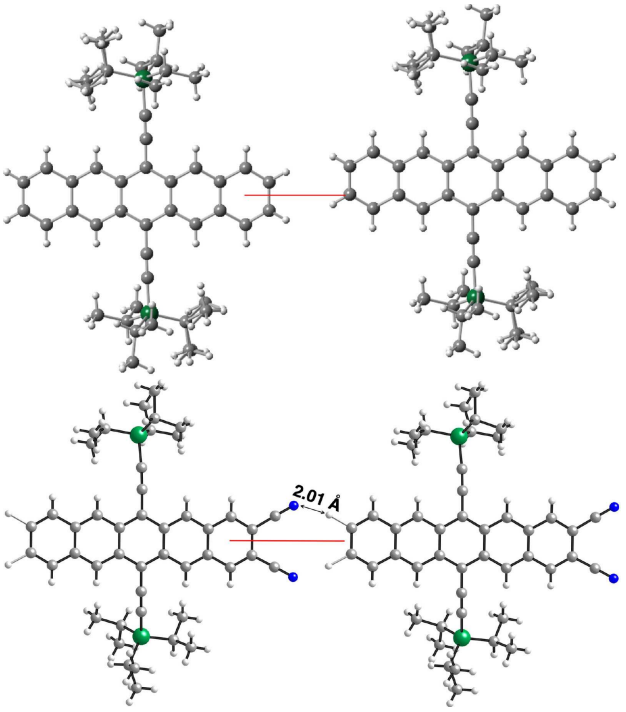

Figure 1. End-to-end acene interactions comparing TIPS pentacene (*top*) and 2,3-dicyano TIPS pentacene (*bottom*). Horizontal red lines are a guide to the eye showing short-axis slip in the solid state.

This 1D tape motif is promising, as it can still form the 2D 'brickwork' arrangement with a proven record in high-performance transistor materials, with the electron deficient rings showing impressive close contacts in the π-stacking direction (as close as 3.34 Å, *Figure 2*, *top*), suggesting potential for good charge transport. While π-overlap in this derivative is excellent, it performed very poorly as an acceptor in polymer solar cells. Looking more broadly at the overall crystal structure, we see that the surface of the growing crystal exposes only the insulating solubilizing groups – the donor polymer has minimal contact with the electronically active core of the acceptor molecule, severely inhibiting the photo-induced electron transfer process necessary for photovoltaic per-

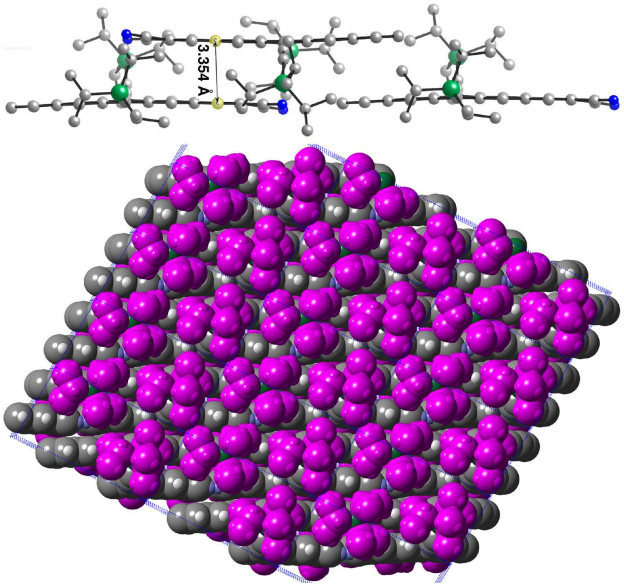

Figure 2. Strong π-stacking interaction between cyanopentacene cores (*top*), measured as a distance between aromatic planes. Note that the largest crystal faces (crystallographic a,b plane) show insulating hydrocarbon (in purple) blocking access to the active chromophores below.

formance (*Figure 2*, *bottom*). However, this crystal packing arrangement should show more potential in field-effect transistors; unfortunately, the dicyano pentacene LUMO energy (−3.64 eV) is not sufficient to allow air-stable operation as an electron-transporting transistor material,[11] and its HOMO energy (−5.45 eV) is too high to allow efficient injection of holes for p-type behavior. We were thus interested to see if less electron-withdrawing π-electron-rich substituents could be used to induce this tape-like crystal packing motif.

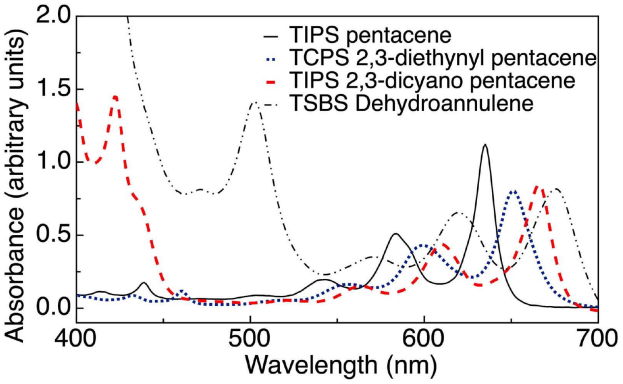

Figure 3. Absorption spectra of silylethyne-functionalized acenes with no substituents (**TIPS pentacene**), ethyne substituents (**TCPS DEP**), and nitrile substituents (**TIPS DCP**), along with the dehydroannulene **TSBS DHA**.

Results and Discussion

We reasoned that an ethyne functional group was the most logical starting point to explore impact on crystal packing, due to the similarity in size between an alkyne and a nitrile. The synthesis of these ethynylpentacenes is straightforward, since the same 2,3-diiodo silylethyne substituted pentacenes required for synthesis of the dinitriles provide ideal starting materials for the palladium-catalyzed coupling of trimethylsilylacetylene. Subsequent careful selective desilylation by treatment with potassium carbonate in methanol yielded four 2,3-diethynyl pentacenes (**DEP**s) in reasonable yield (solubilized by central triisopropylsilyl ethynyl (**TIPS DEP**, *Cambridge Structural Database* (*CSD*) registry number 1891422), triisobutylsilylethynyl (**TIBS DEP**), tri *sec*-butylsilyl (**TSBS DEP**) or tricyclopentylsilyl (**TCPS DEP**, *CSD* registry number 1891423) groups). These terminal alkyne functionalized pentacenes were stable in the crystalline state, and crystal growth from hexanes or acetone yielded material suitable for X-ray structure determination.

Photophysical characterization showed the **DEP**s possess an optical gap slightly blue-shifted compared to that observed in cyanopentacenes, and both of these pentacene classes show slightly red-shifted absorptions compared to the parent TIPS pentacene (*Figure 3*). These new materials were also characterized electrochemically, to determine relative orbital energy levels. The approximate HOMO energy value was calculated from the solution electrochemistry data using ferrocene as an internal reference,[12] yielding a value of −5.3 eV. This value is similar to many other hole-transporting materials, suggesting that charge injection will not be an issue for device performance, provided other critical criteria can be met.

These new pentacenes yielded a variety of crystal packing motifs, though none of these adopted the 1D tape arrangement found in the corresponding dinitriles. Rather than aromatic C–H-π interactions, the bulk of these materials adopted configurations showing strong *alkyne* C–H-π bonding, as shown for an exemplary (tricyclopentylsilyl) derivative in *Figure 4* (a slightly different alkyne C–H-π motif found in **TIPS DEP**, where the acenes are roughly perpendicular rather than co-planar, is shown in *Figure S1* in the *Supplementary Information*).

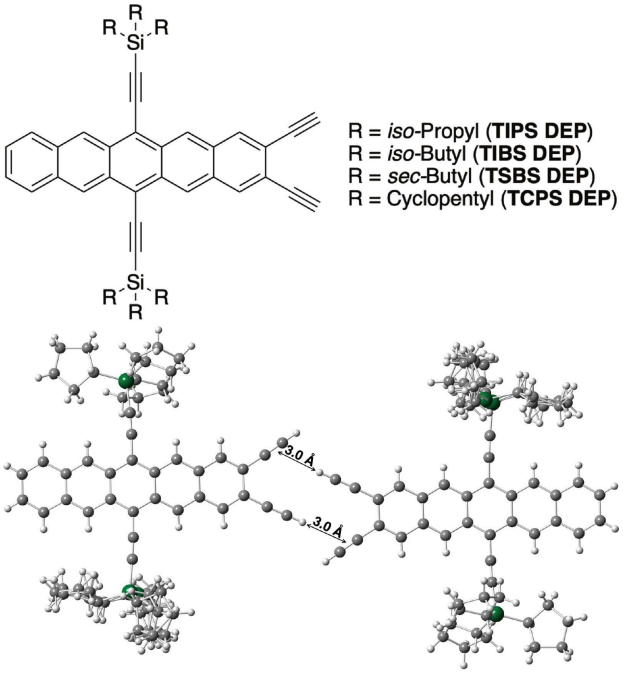

Figure 4. DEP molecules prepared for this study (*top*) and crystal motif for a typical diethynyl pentacene (**TCPS DEP**) showing close intermolecular C–H-π_{alkyne} interactions.

These hydrogen/alkyne interactions are relatively common, and the H–C distances found here on the order of 3 Å falls within the range (2.9–3.1 Å) typically observed for such interactions.[13] Thus, rather than the head-to-tail structures seen with the dinitriles, all of the diethynyl pentacenes adopt head-to-head motifs. None of these derivatives exhibit the types of long-range π-stacking interactions that would make them suitable for electronic applications, and the insulating solubilizing groups still consume the bulk of the area of all crystalline facets.

To increase the ratio of aromatic surface to solubilizing hydrocarbon, we converted these *o*-diethynyl arenes to dehydroannulenes (DHAs) by simple oxidative coupling. Dehydroannulenes continue to arise as interesting scaffolds for organic materials,[14] and dehydrobenzo[18]annulenes in particular have been extensively explored for their unusual photophysical,[15–20] redox,[21–23] nonlinear optical,[24] and most relevant to this work, self-assembly properties,[25,26] but to the best of our knowledge have not been investigated for electronic devices such as photovoltaics. Cyclization of the ethynyl pentacenes was performed using standard *Hay* coupling conditions.[27] Attempted cyclotrimerization of **TIPS DEP** was unsuccessful – the material precipitated from solution as an acyclic dimer, and was resistant to further elaboration due to poor solubility. However, pentacene-fused DHAs solubilized with triisobutylsilylethynyl (**TIBS DHA**, *CSD* registry number 1891425) and tri *sec*-butylethynyl (**TSBS DHA**, *CSD* registry number 1891424) groups were sufficiently soluble and stable for isolation, and were suitably crystalline for structure determination.

The absorption spectra of these aromatic macrocycles (*Figure 3*) show the typical vibronic progression of pentacene, slightly red-shifted compared to the acyclic starting material, as well as a sharp transition at *ca.* 500 nm, likely arising from the annulene chromophore red-shifted by the appended pentacenes.[28] While reasonably stable in the solid state, manipulations of solutions of these DHAs were performed with shielding from laboratory light. Even relatively dilute solutions shielded from oxygen showed a half-life of approximately 18 hours (as determined by UV/Vis absorption studies – see *Figure S2* in the *Supplementary Information*). Electrochemical analysis (see *Figure S3* in the *Supplementary Information*) showed a reversible reduction at −1.3 V *vs.* the ferrocene/ferrocenium couple, leading to an estimated LUMO energy of −3.5 eV, which is similar to that of other pentacene-based acceptors used successfully in blends with poly(thiophene)s.[29] The DHAs showed a quasi-reversible reduction at −1.8 V, and a poorly reversible oxidation at 0.48 V *vs.* ferrocene.

While crystallographic analysis of **TIBS DHA** and **TSBS DHA** certainly confirm the large, planar structure (see *Figure 5* (*top*) for the thermal ellipsoid plot of

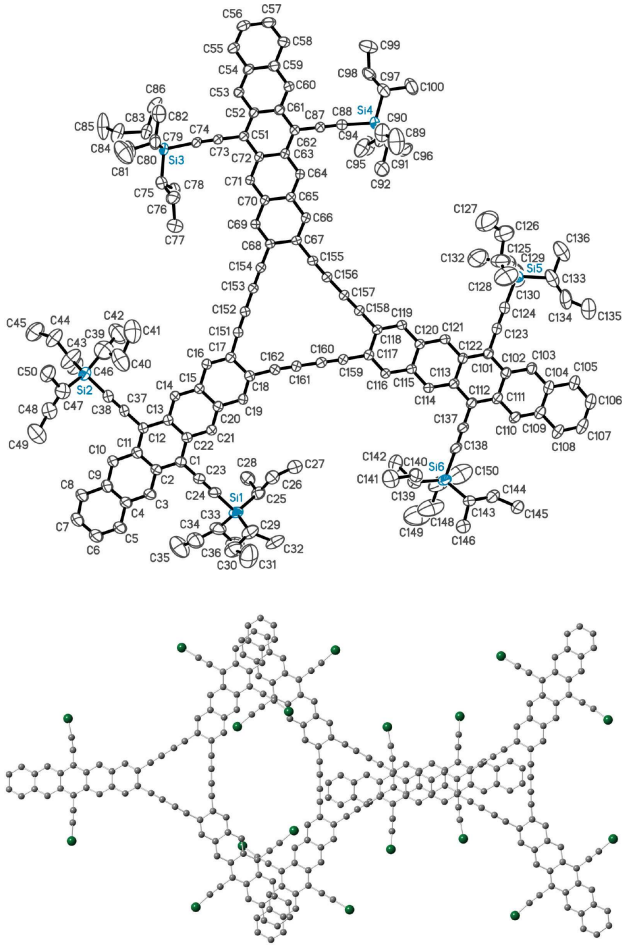

Figure 5. Thermal ellipsoid plot of **TSBS DHA** (*top*) and crystal packing of this molecule showing strong pentacene -pentacene π-stacking interactions (*bottom*).

TSBS DHA), more enticingly both of these derivatives show extensive three-dimensional π-stacking interactions. As shown at the bottom of *Figure 5*, pentacene-pentacene stacking interactions dominate the crystal-packing motif, with C–C contacts as close as 3.42 Å, suggesting strong intermolecular communication. The potential for electronic coupling (and thus, charge transport) in three dimensions, along with suitable LUMO energies and sufficient solubility and stability for spin-coating, led us to explore the use of these DHAs as acceptors in bulk-heterojunction OPVs.

Devices were constructed in a conventional configuration, starting with a cleaned, patterned indium tin oxide substrate coated with poly(ethylenedioxythiophene): poly(styrenesulfonate), **PEDOT:PSS**. Fifteen mg of **TSBS DHA** was blended with an equal mass of **P3HT** in 1.25 mL of chlorobenzene, and the solution stirred until both compounds had completely dissolved. The solution was then spin-coated onto the substrate (1000 rpm, 60 s) and allowed to dry. The cathode (Al) was deposited in an 80 nm thick layer under high vacuum. The resulting devices were then thermally annealed at 150 °C. The blend of **TSBS DHA** and **P3HT** did indeed form a working photovoltaic cell, although performance was poor and device stability was an issue. The best-performing devices showed an overall power-conversion efficiency of 0.02%, with an open-circuit voltage of 0.6 V and short-circuit current for the best devices approaching 0.2 mA/cm^2. Poor fill factors (between 20 and 30%) suggest that further optimization of blend ratio, casting solvent, or process conditions could yield performance improvements, but the low stability suggests molecule structural modifications should be performed before extensive optimization takes place. We have developed several approaches to improve the stability of acene-based materials, such as substitution with heteroaromatic components or fluorination, or even the use of slightly smaller (*e.g.*, tetracene) acenes in dehydroannulene forms. We are currently exploring all of these approaches.

Conclusions

In summary, we demonstrated how subtle changes in structure and electronics can elicit alternative (weak) intermolecular interactions that can in turn drive pentacene chromophores to adopt different crystal packing motifs. In particular, switching from nitrile (CN) to terminal alkyne (C_2H) groups changed the secondary interactions from head-to-tail to head-to-head. Cyclization of the *o*-arenediyne pentacenes yielded dehydro[18]annulenes, which X-ray crystallographic analysis showed exhibited long-range 3-dimensional π-stacking interactions. Sample photovoltaic devices formed using these annulenes as acceptors did function as expected, albeit with poor overall performance. However, these results suggest that more stable dehydroannulenes may serve as a viable platform to achieve the 3-dimensional electronic coupling between acceptors that are required for high-efficiency organic photovoltaics.

Experimental Section

Materials and Methods

All solvents were purchased from *Pharmco-Aaper*, *Fisher Scientific*, *Alfa Aesar*, and *Sigma-Aldrich*. Trimethylsilylacetylene was purchased from *Gelest*, All other catalysts, anhydrous tetrahydrofuran (THF) and reagents were purchased from *Sigma-Aldrich*. Chromatography was performed on silica gel (60 Å, 40–63 μm) purchased from *SiliCycle*. Visible-NIR spectra were recorded on an *HP 8453* or a *Thermo-Fisher Scientific Evolution 60* spectrophotometer. NMR spectra were recorded on a *Varian Inova 400* MHz spectrometer. Mass spectra were recorded in MALDI mode on a *Bruker Daltonics Autoflex* MALDI-TOFMS. Combustion analyses were done by *Midwest Microlab* (Indianapolis, IN). Melting points of precursory compounds were measured with a standard capillary melting point apparatus. Melting points of some larger compounds were additionally determined by differential scanning calorimetry using a *Thermo-Fisher Scientific DSCQ100* with a heating rate of 10 °C/min under nitrogen. DSC melting points are given as the endothermic peak onset. Electrochemistry was performed with a *BASi Epsilon model E2* potentiostat. Measurements were taken in a 0.1 M NBu_4PF_6 solution of methylene chloride (degassed with N_2) with a Pt button working electrode and silver wire reference electrode. Ferrocene was subsequently added as an internal standard. Diiodopentacenes were prepared according to published procedures.[8]

X-Ray Characterization

X-Ray data were collected on either a *Nonius kappaCCD* or a *Bruker-Nonius X8 Proteum CCD* diffractometer using MoK_α or CuK_α radiation, respectively. The structures were solved using SHELXS and refined using SHELXL from the SHELX[30,31] program package. Molecular fragment editing was performed using the XP program of SHELXTL.[30] All non-hydrogen atoms were refined with anisotropic displacement parameters. H atoms were found in difference *Fourier* maps and subsequently placed in idealized positions within constrained distances of the attached atom.

Diethynyl Pentacene (DEP) *Synthesis*

TIPS DEP: In a 25 mL round-bottom flask was combined 10 mL THF, 2,3-diiodo TIPS pentacene (0.69 g, 0.77 mmol), and 1.6 mL triethylamine. The solution was sparged with nitrogen for 15 min before adding $Pd(PPh_3)_2Cl_2$ (0.036 mmol, 26 mg, 0.047 equiv.),

CuI (0.073 mmol, 14 mg, 0.094 equiv.), and trimethylsilylacetylene (0.210 g, 2.19 mmol, 2.80 equiv.). The reaction vessel was sealed and heated at 30 °C overnight. Thin layer chromatography in hexanes showed that the product had nearly the same R_f as the starting material. Investigation with UV/Vis spectroscopy in hexanes showed the starting diiodo compound had a long-wavelength absorption maximum at 649 nm, whereas the reaction solution had a slight red shift to 652 nm. Appearing complete, the solvent was removed, and the material was eluted through a silica gel plug with hexanes/dichloromethane 9:1 to give 0.74 g (>100% yield). This product was carried on without further purification by dissolving the product in 150 mL methanol and *ca.* 40 mL THF, adding 200 mg K_2CO_3, and stirring for 1 h. The mixture was filtered, and the solvent evaporated before being eluted through a silica gel plug with hexanes/dichloromethane 9:1 to give 440 mg of product. This was recrystallized from 15–20 mL boiling hexanes to give 322 mg fine needles, 61% over two steps. Larger X-ray quality crystals were grown from $CHCl_3$/MeOH by solvent diffusion in an NMR tube over *ca.* 1 week. ^{1}H-NMR (400 MHz, $CDCl_3$): 9.30 (*s*, 2 H); 9.21 (*s*, 2 H); 8.19 (*s*, 2 H); 7.98 (*dd*, *J*=6.4, 2.8, 2 H); 7.44 (*dd*, *J*=6.4, 2.8, 2 H); 3.46 (*s*, 2 H); 1.38 (*s*, 42 H). ^{13}C-NMR (100 MHz, $CDCl_3$): 134.6; 132.8; 131.3; 131.1; 130.4; 128.9; 127.0; 126.7; 126.6; 120.5; 119.1; 108.1; 104.4; 82.5; 81.6; 19.2; 11.9. LDI-MS 686.4 (M^+). HR-MS: 686.3759 ($C_{48}H_{54}Si_2^+$; calc. 686.3764).

TSBS DEP: Prepared following the same procedure as above, starting with 0.730 g of 2,3-diiodo TSBS pentacene. The final DEP was eluted through a silica gel plug with hexanes followed by hexanes/dichloromethane 12:1 to yield 360 mg of product, which was recrystallized from 5 mL acetone to give 270 mg of tiny blue flakes/needles, 47% yield over two steps. ^{1}H-NMR (400 MHz, $CDCl_3$): 9.29 (*s*, 2 H); 9.20 (*s*, 2 H); 8.18 (*s*, 2 H); 7.98 (*dd*, *J*=6.6, 3.2, 2 H); 7.45 (*dd*, *J*=6.6, 3.2, 2 H); 3.46 (*s*, 2 H); 2.21–1.95 (*m*, 6 H); 1.72–1.48 (*m*, 6 H); 1.34 (*d*, *J*=7.2, 18 H); 1.24–1.19 (*m*, 6 H); 1.15 (*t*, *J*=7.2, 18 H). ^{13}C-NMR (100 MHz, $CDCl_3$): 134.6; 132.8; 131.3; 131.1; 130.5; 128.9; 127.0; 126.7; 126.6; 120.5; 119.2; 109.2; 104.5; 82.5; 81.6; 25.93; 25.90; 19.5; 15.00; 14.97; 14.1. LDI-MS: 770.5 (M^+). HR-MS: 770.4699 ($C_{54}H_{66}Si_2^+$; calc. 770.4703).

TIBS DEP: Prepared following the procedure used for **TIPS DEP**, starting with 0.500 g of 2,3-diiodo TIBS pentacene. Due to the lability of the TIBS group, the desilylation reaction was carefully monitored by TLC (hexanes) every 10 min and was shown to be complete after 50 min. The product was purified by elution through a silica gel plug with hexanes/dichloromethane 12:1 to give 550 mg of product, which was recrystallized from 2.8 mL heptane (105 °C) to give 305 mg of large blue blocks, 40% yield. ^{1}H-NMR (400 MHz, $CDCl_3$): 9.28 (*s*, 2 H); 9.19 (*s*, 2 H); 8.20 (*s*, 2 H); 7.99 (*dd*, *J*=6.6, 3.2, 2 H); 7.46 (*dd*, *J*=6.6, 3.2, 2 H); 3.46 (*s*, 2 H); 2.21 (*nonet*, *J*=6.6, 6 H); 1.22 (*d*, *J*=6.6, 36 H); 0.99 (*d*, *J*=6.6, 12 H). ^{13}C-NMR (100 MHz, $CDCl_3$): 134.4; 132.8; 131.3; 131.1; 130.5; 128.8; 128.6; 126.9; 126.6; 120.6; 119.2; 110.9; 104.4; 82.5; 81.6; 26.8; 25.7; 25.6. LDI-MS: 770.5 (M^+). HR-MS: 770.4705 ($C_{54}H_{66}Si_2^+$; calc. 770.4703).

TCPS DEP: Prepared following the procedure used for **TIPS DEP**. The crude material from the desilylation was eluted through a silica column with hexanes/dichloromethane 9:1 to give 0.05 g of blue solid, 58% yield. X-ray quality crystals were grown from 1,2-dichloroethane. ^{1}H-NMR (400 MHz, $CDCl_3$): 9.29 (*s*, 2 H); 9.21 (*s*, 2 H); 8.18 (*s*, 2 H); 7.97 (*dd*, *J*=6.54, 3.15, 2 H); 7.42 (*dd*, *J*=6.71, 3.04, 2 H); 3.44 (*s*, 2 H); 1.54 (*s*, 2 H); 1.48–1.23 (*m*, 46 H); 0.94–0.83 (*m*, 4 H); 0.66 (*s*, 2 H). ^{13}C-NMR (100 MHz, $CDCl_3$): 134.5; 132.8; 131.3; 131.0; 130.5; 128.8; 127.0; 126.7; 126.6; 120.5; 119.2; 108.8; 103.5; 82.5; 81.6; 29.6; 27.3; 24.1 LDI-MS: 770.5 (M^+). HR-MS: 842.4698 ($C_{60}H_{66}Si_2^+$; calc. 842.4703).

Dehydroannulene (DHA) *Synthesis*

TIBS DHA: In a 250-mL round-bottom flask was combined 110 mg (0.143 mmol) 2,3-diethynyl TIBS pentacene (**TIBS DEP**), 35 mL acetone, and 0.2 mL *Hay* catalyst. (*Hay* catalyst was prepared in a separate small flask by combining 50 mg CuCl, 1.5 mL acetone, and 10 drops of tetramethylethylenediamine (TMEDA) and stirring for 30 min.) The mixture was stirred rapidly open to air such that the solution splashed in the flask and kept the solution saturated with air (O_2). The initial blue pentacene solution gradually became greenish over 10–20 min, and eventually more brownish as the mixture stirred overnight. The next day, remaining solvent was evaporated and a silica gel plug was run eluting with hexanes/CH_2Cl_2 9:1 giving a very crude separation. A flash column was then run with a gradual linear ramp of 1% to 10% CH_2Cl_2 in hexanes over 20 min. A small blue band of remaining TIBS-2,3-diethynylpentacene eluted first, followed by greenish and greenish-brown spots which nearly co-eluted. Given that the brownish spot appeared most plentiful, fractions containing the most pure brownish spot

were combined and evaporated. The residue was dissolved in approx. 10 mL hexanes and 5 mL CH_2Cl_2 in a 50 mL round-bottom flask at room temperature and left in the dark to evaporate slowly over the weekend, producing *ca.* 15 mg of X-ray quality crystals. ^{1}H-NMR (400 MHz, $CDCl_3$): 9.29 (*s*, 6 H); 9.21 (*s*, 6 H); 8.29 (*s*, 6 H); 8.00 (*dd*, J = 6.4, 3.2, 6 H); 7.47 (*dd*, J = 6.4, 3.2, 6 H); 2.24 (*nonet*, J = 6.8,18 H); 1.26 (*d*, J = 6.8, 108 H); 1.03 (*d*, J = 6.8, 36 H). LDI-MS: 2305 (M^-). UV/Vis (CH_2Cl_2): 471, 502 (sh), 571, 619 (sh), 676 (sh).

TSBS DHA: In a 50-mL round-bottom flask was combined 132 mg (0.144 mmol) TSBS-2,3-diethynylpentacene, 3.2 mL acetone, and 0.2 mL *Hay* catalyst (prepared as described above). The mixture was stirred rapidly open to air overnight. After evaporation of solvent, the residue was eluted through a thin pad of silica gel using hexanes/CH_2Cl_2 9:1 to give a very crude separation. A flash column was then run with a gradual linear ramp of 1% to 10% CH_2Cl_2 in hexanes over 20 min. A small blue band of remaining TSBS-2,3-diethynylpentacene eluted first, followed by a greenish-brown spot. The solvent was evaporated, and the residue was dissolved in approx. 10 mL hexanes and 5 mL CH_2Cl_2 in a 50-mL round-bottom flask at room temperature and left in the dark to evaporate slowly, producing X-ray quality crystals, 34 mg, 26% yield. We note that better quality crystals could be prepared by layering methanol over chloroform in an NMR tube. ^{1}H-NMR (400 MHz, $CDCl_3$): 9.33 (*s*, 6 H); 9.22 (*s*, 6 H); 8.28 (*s*, 6 H); 8.00 (*dd*, J = 6.4, 3.2, 6 H); 7.47 (*dd*, J = 6.4, 3.2, 6 H); 2.07 (*m*, 18 H); 1.61 (*m*, 18 H); 1.42 (*d*, J = 7.2, 54 H); 1.22 (*t*, J = 7.2, 54 H); 1.07 (*m*, 18 H). ^{13}C-NMR (100 MHz, $CDCl_3$): 135.4; 132.9; 131.5; 131.2; 130.4; 128.9; 127.4; 126.8; 126.7; 120.3; 119.4; 109.3; 104.6; 82.2; 79.2; 26.0; 19.5; 15.1; 14.2. LDI-MS: 2305.4 (M^-).

Acknowledgements

J. E. A., *S. R. P.*, and *E. K. H.* thank the U.S. National Science Foundation for support of the synthesis of novel aromatic materials (CHE-1609974) and for diffractometer support funding (MRI: CHE-0319176, CHE-1625732).

Author Contribution Statement

J. E. A. and *Y. L. L.* conceived and designed the experiments and wrote the manuscript. *M. J. B.* and *E. K. H.* synthesized and characterized the materials, while *A. K. H.* fabricated and analyzed the photovoltaics. *S. R. P.* performed crystallographic analysis.

References

[1] J. L. Brédas, J. P. Calbert, D. A. da Silva Filho, J. Cornil, 'Organic semiconductors: A theoretical characterization of the basic parameters governing charge transport', *Proc. Natl. Acad. Sci. USA* **2002**, *99*, 5804–5809.

[2] Z.-F. Yao, J.-Y. Wang, J. Pei, 'Control of π-π Stacking via Crystal Engineering in Organic Conjugated Small Molecule Crystals', *Cryst. Growth Des.* **2018**, *18*, 7–15.

[3] S. Kim, B. Kim, J. Lee, H. Shin, Y.-I. Park, J. Park, 'Design of fluorescent blue light-emitting materials based on analyses of chemical structures and their effects', *Mater. Sci. Eng. Rep.* **2016**, *99*, 1–22.

[4] Y.-T. Fu, C. Risko, J.-L. Brédas, 'Intermixing at the Pentacene-Fullerene Bilayer Interface: A Molecular Dynamics Study', *Adv. Mater.* **2013**, *25*, 878–882.

[5] O. Kwon, V. Coropceanu, N. E. Gruhn, J. C. Durivage, J. G. Laquindanum, H. E. Katz, J. Cornil, J. L. Brédas, 'Characterization of the molecular parameters determining charge transport in anthradithiophene', *J. Chem. Phys.* **2004**, *120*, 8186–8194.

[6] J. E. Anthony, 'The Larger Acenes: Versatile Organic Semiconductors', *Angew. Chem. Int. Ed.* **2008**, *47*, 452–483.

[7] J. E. Anthony, D. L. Eaton, S. R. Parkin, 'A Road Map to Stable, Soluble, Easily Crystallized Pentacene Derivatives', *Org. Lett.* **2002**, *4*, 15–18.

[8] Y. Shu, Y.-F. Lim, Z. Li, B. Purushothaman, R. Hallani, J. E. Kim, S. R. Parkin, G. G. Malliaras, J. E. Anthony, 'A survey of electron-deficient pentacenes as acceptors in polymer bulk-heterojunction solar cells', *Chem. Sci.* **2011**, *2*, 363–368.

[9] C. R. Swartz, S. R. Parkin, J. E. Bullock, J. E. Anthony, A. C. Mayer, G. G. Malliaras, 'Synthesis and Characterization of Electron-Deficient Pentacenes', *Org. Lett.* **2005**, *7*, 3163–3166.

[10] J.-Y. Le Questel, M. Berthelot, C. Laurence, 'Hydrogen-bond acceptor properties of nitriles: a combined crystallographic and *ab initio* theoretical investigation', *J. Phys. Org. Chem.* **2000**, *13*, 347–358.

[11] J. E. Anthony, A. Facchetti, M. Heeney, S. R. Marder, X. Zhan, 'n-Type Organic Semiconductors in Organic Electronics', *Adv. Mater.* **2010**, *22*, 3876–3892.

[12] C. M. Cardona, W. Li, A. E. Kaifer, D. Stockdale, G. C. Bazan, 'Electrochemical Considerations for Determining Absolute Frontier Orbital Energy Levels of Conjugated Polymers for Solar Cell Applications', *Adv. Mater.* **2011**, *23*, 2367–2371.

[13] C. J. McAdam, S. A. Cameron, L. R. Hanton, A. R. Manning, S. C. Moratti, J. Simpson, 'Probing CH-π(alkyne) interactions in a series of ethynylferrocenes', *CrystEngComm* **2012**, *14*, 4369–4383.

[14] E. L. Spitler, C. A. Johnson II, M. M. Haley, 'The Renaissance of Annulene Chemistry', *Chem. Rev.* **2006**, *106*, 5344–5386.

[15] J. A. Marsden, J. J. Miller, L. D. Shirtcliff, M. M. Haley, 'Structure–Property Relationships of Donor/Acceptor-Functionalized Tetrakis(phenylethynyl)benzenes and Bis

(dehydrobenzoannuleno)benzenes', *J. Am. Chem. Soc.* **2005**, *127*, 2464–2476.

[16] X. Zhou, A.-M. Ren, J.-K. Feng, X.-J. Liu, 'Studies on the two-photon absorption properties of trigonal dehydrobenzo [18]annulenes', *Can. J. Chem.* **2004**, *82*, 1172–1178.

[17] A. Bhaskar, R. Guda, M. M. Haley, T. Goodson III, 'Building Symmetric Two-Dimensional Two-Photon Materials *J. Am. Chem. Soc.* **2006**, *128*, 13972–13973.

[18] E. L. Spitler, M. M. Haley, 'Synthesis and Structure–Property Relationships of Donor/Acceptor-Functionalized Bis(dehydrobenzo[18]annuleno)benzenes *Org. Biomol. Chem.* **2008**, *6*, 1569–1576.

[19] S. Anand, O. Varnavski, J. A. Marsden, M. M. Haley, H. B. Schlegel, T. Goodson III, 'Optical Excitations in Carbon Architectures Based on Dodecadehydrotribenzo[18]annulene*J. Phys. Chem. A* **2006**, *110*, 1305–1318.

[20] C. Mang, C. Liu, P. Liu, J. Zi, J. Zhou, X. Zhao, K. Wu, 'Excited electronic states of dehydro[18]annulene and dehydrobenzo[18]annulene', *J. Mol. Struct.: THEOCHEM* **2008**, *857*, 27–32.

[21] C. R. Parker, K. Lincke, M. A. Christensen, K. Lušpai, P. Rapta, T. J. Sørensen, T. J. Morsing, L. Du, H. G. Kjaergaard, O. Hammerich, F. Diederich, M. B. Nielsen, 'On the association of neutral and cationic tris(tetrathiafulvaleno)dodecadehydro[18]annulenes', *Org. Biomol. Chem.* **2016**, *14*, 425–429.

[22] T. Nishinaga, Y. Miyata, N. Nodera, K. Komatsu, 'Synthesis and properties of *p*-benzoquinone-fused hexadehydro[18] annulenes', *Tetrahedron* **2004**, *60*, 3375–3382.

[23] R. S. Iglesias, C. G. Claessens, M. Á. Herranz, T. Torres, 'Subphthalocyanine-Dehydro[18]annulenes', *Org. Lett.* **2007**, *9*, 5381–5384.

[24] A. Sarkar, J. J. Pak, G. W. Rayfield, M. M. Haley, 'Nonlinear optical properties of dehydrobenzo[18]annulenes: Expanded two-dimensional dipolar and octupolar NLO chromophores', *J. Mater. Chem.* **2001**, *11*, 2943–2945.

[25] K. Tahara, C. A. Johnson II, T. Fujita, M. Sonoda, F. De Schryver, S. De Feyter, M. M. Haley, Y. Tobe, 'Synthesis of Dehydrobenzo[18]annulene Derivatives and Formation of Self-Assembled Monolayers: Implication of Core Size on Alkyl Chain Interdigitation', *Langmuir* **2007**, *23*, 10190–10197.

[26] K. Tahara, S. Lei, J. Adisoejoso, S. De Feyter, Y. Tobe, 'Supramolecular surface-confined architectures created by self-assembly of triangular phenylene–ethynylene macrocycles *via* van der Waals interaction', *Chem. Commun.* **2010**, *46*, 8507–8525.

[27] A. S. Hay, 'Oxidative Coupling of Acetylenes. II', *J. Org. Chem.* **1962**, *27*, 3320–3321.

[28] B. Zimmermann, G. Baranović, Z. Štefanić, M. Rožman, 'Spectroscopic properties of macrocyclic oligo(phenyldiacetylenes)-II. Synthesis and theoretical study of diacetylenic dehydrobenzoannulene derivatives with weak electron-donor and -acceptor groups', *J. Mol. Struct.* **2006**, *794*, 115–124.

[29] Y.-F. Lim, Y. Shu, S. R. Parkin, J. E. Anthony, G. G. Malliaras, 'Soluble n-type pentacene derivatives as novel acceptors for organic solar cells', *J. Mater. Chem.* **2009**, *19*, 3049–3056.

[30] G. M. Sheldrick, 'A short history of *SHELX*', *Acta Crystallogr., Sect. A* **2008**, *64*, 112–122.

[31] G. M. Sheldrick, 'Crystal structure refinement with *SHELXL*', *Acta Crystallogr. Sect. C* **2015**, *71*, 3–8.

Received January 28, 2019
Accepted March 5, 2019